Imaging of Friedel Oscillation Patterns of Two-Dimensionally Accumulated Electrons at Epitaxially Grown InAs(111)*A* Surfaces

K. Kanisawa,[1] M. J. Butcher,[1,2] H. Yamaguchi,[1] and Y. Hirayama[1,3]

[1]*NTT Basic Research Laboratories, 3-1 Wakamiya, Morinosato, Atsugi, Kanagawa 243-0198, Japan*
[2]*School of Physics and Astronomy, University of Nottingham, Nottingham NG7 2RD, United Kingdom*
[3]*CREST-JST, 4-1-8 Honmachi, Kawaguchi, Saitama 331-0012, Japan*

(Received 3 May 2000; revised manuscript received 26 December 2000)

The local density of states (LDOS) at the epitaxially grown InAs surface on a GaAs(111)*A* substrate were characterized using low-temperature scanning tunneling microscopy. Using dI/dV signal mapping, LDOS standing waves were clearly imaged at point defects and within nanostructures. Measurement of the wavelength as a function of bias voltage showed a nonparabolic dispersion relation for the conduction band. The observed wave features originate from the Friedel oscillations of the two-dimensional electron gas in the semiconductor surface accumulation layer.

DOI: 10.1103/PhysRevLett.86.3384 PACS numbers: 73.61.Ey, 68.37.Ef, 72.10.Fk, 73.22.–f

Quantum mechanical understanding of electron behavior in semiconductors is important in the mesoscopic regime. This is because the electron waves are dramatically affected by small defect concentrations due to long range screening phenomena [1]. Recently, the wave phenomena have been studied by using scanning tunneling microscopy (STM). On the noble metal surfaces, clear standing waves of a two-dimensional electron gas (2DEG) in the Shockley surface state bands have been observed [2–4]. The only semiconductor surfaces to show interference effects are cleaved (110) surfaces with three-dimensional electron gas (3DEG) [5,6] and a Si(001) surface with one-dimensional electron gas (1DEG) [7]. Until now, there is no report on a semiconductor 2DEG using STM, although such a 2DEG is important as it at the core of a field-effect transistor. The semiconductor 2DEG is also important as an ideal two-dimensional system with flexible carrier control via gates and doping, although the 2DEG on the noble metal surfaces are not ideal [4].

In this Letter, we present results on the oscillatory 2DEG local density of states (LDOS) quantized in the accumulation layer at an epitaxial InAs(111)*A* surface using low-temperature STM (LT-STM).

On a n^+-GaAs(111)*A* substrate, a 100–200 nm thick undoped InAs was grown in a layer-by-layer growth mode [8] by molecular beam epitaxy (MBE). The sample was then transferred to the LT-STM in ultrahigh vacuum and cooled. Topographic images were obtained in constant current (0.2–0.4 nA) mode at 5.3–23.5 K. We applied a modulation (5–7 mV rms at 400–600 Hz) to the bias voltage V (tip neutral) during the imaging and detected the dI/dV signal simultaneously using a lock-in amplifier.

Figure 1(a) shows the typical $(dI/dV)/(I/V)$-V characteristics measured on the epitaxial InAs(111)*A* surface by scanning tunneling spectroscopy. Obtained $E_{F,\mathrm{InAs}} - E_c$ about 0.2 eV is comparable to a reported 0.21 ± 0.05 eV [9]. Here, $E_{F,\mathrm{InAs}}$ and E_c are the Fermi level of InAs and the bottom of the conduction band, respectively. From the magnetotransport measurement, the sheet electron density of a 212 nm thick epitaxial InAs layer was measured to be 3.2×10^{12} cm^{-2} at low temperature. If all the electrons are 3DEG, $E_{F,\mathrm{InAs}} - E_c$ is about 0.026 eV (Fermi wavelength $\lambda_{F,0} = 38$ nm), which is much smaller than the measured 0.2 eV. The donor-type surface state density at the InAs(111)*A* substrate was reported to be about 8×10^{11} cm^{-2} (0.1% of a monolayer) [10]. Such a surface state density causes 2DEG accumulation at the surfaces [9,10]. Since the epitaxial InAs on the lattice-mismatched GaAs(111)*A* substrate must have more defects, such a film strongly tends to have the 2DEG at the surface [Fig. 1(b)]. This situation differs from that of the 3DEG dominance at the clean InAs(110) surface [6,12].

The LDOS probed at $V < 0$ V below the bulk E_c on the InAs(111)*A* surface is only the 2DEG LDOS which is separated from bulk states. At this condition, we observed wavy patterns of many concentric and isotropic circular corrugations at the surface state sites (Fig. 2). In the fast Fourier transforms (FFT) power spectra of the dI/dV images, a larger wave number was obtained from higher electron energy E.

The external electric fields due to the work function difference $\Delta\Phi(= \Phi_{\mathrm{tip}} - \Phi_{\mathrm{InAs}})$ and V modifies the band diagram below the tip [Fig. 1(b)]. We define the surface potential due to band bending as $\phi_s(\Delta\Phi, V) \equiv \phi_{s,0} - \alpha(\Delta\Phi + eV)$ $(0 \le \alpha \le 1)$. Here, $\phi_{s,0}$ is the bending at $V = 0$ V. If there is a high enough surface state density to trap all externally accumulated electrons, these electrons completely screen the local effect with no extrinsic field penetration into the InAs layer, i.e., $\alpha = 0$ (case I). However, if the surface state density is too low to trap such electrons, the external field modifies the potential features. The maximum modification occurs when the whole of $\Delta\Phi + eV$ $(\equiv \Delta U)$ is applied to the surface, i.e., $\alpha = 1$ (case II). Present results must be between these two limits. Schrödinger's equation and Poisson's equation were solved consistently considering parabolic band bending at the surface and the interface. In case I,

 0031-9007/01/86(15)/3384(4)$15.00

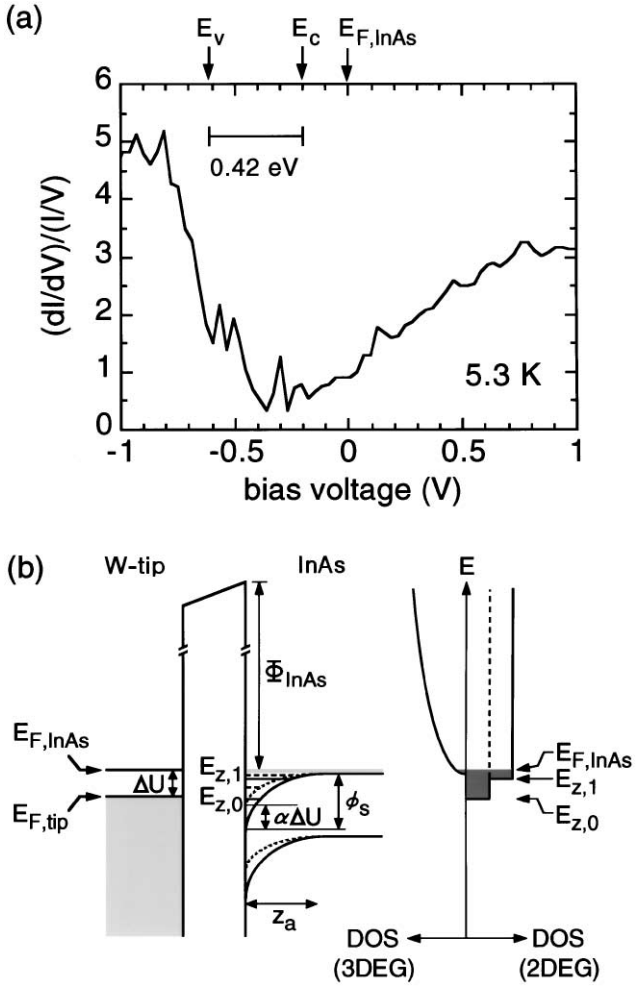

FIG. 1. (a) $(dI/dV)/(I/V)$-V characteristics measured on the InAs(111)A surface at 5.3 K. E_c, E_v, $E_{F,\mathrm{InAs}}$, and the band gap E_g (0.42 eV) are shown. (b) Energy band profile at the surface with tip approached. $E_{F,\mathrm{tip}}$ is Fermi level position of the tip. Solid (dashed) curve is the band diagram at $V \neq 0$ V ($V = 0$ V). $\Delta\Phi \equiv 0$ eV. ϕ_s is the surface potential. $E_{z,0}$ and $E_{z,1}$ are 2DEG subbands. Hatched DOS region shows occupied states. For calculation, we included the accumulated 2DEG at the InAs/GaAs interface (not shown). Electron effective mass $m^* = 0.04m_0$ [11] and significant amount of positive charge in InAs layer (for satisfying the charge neutrality condition) are assumed.

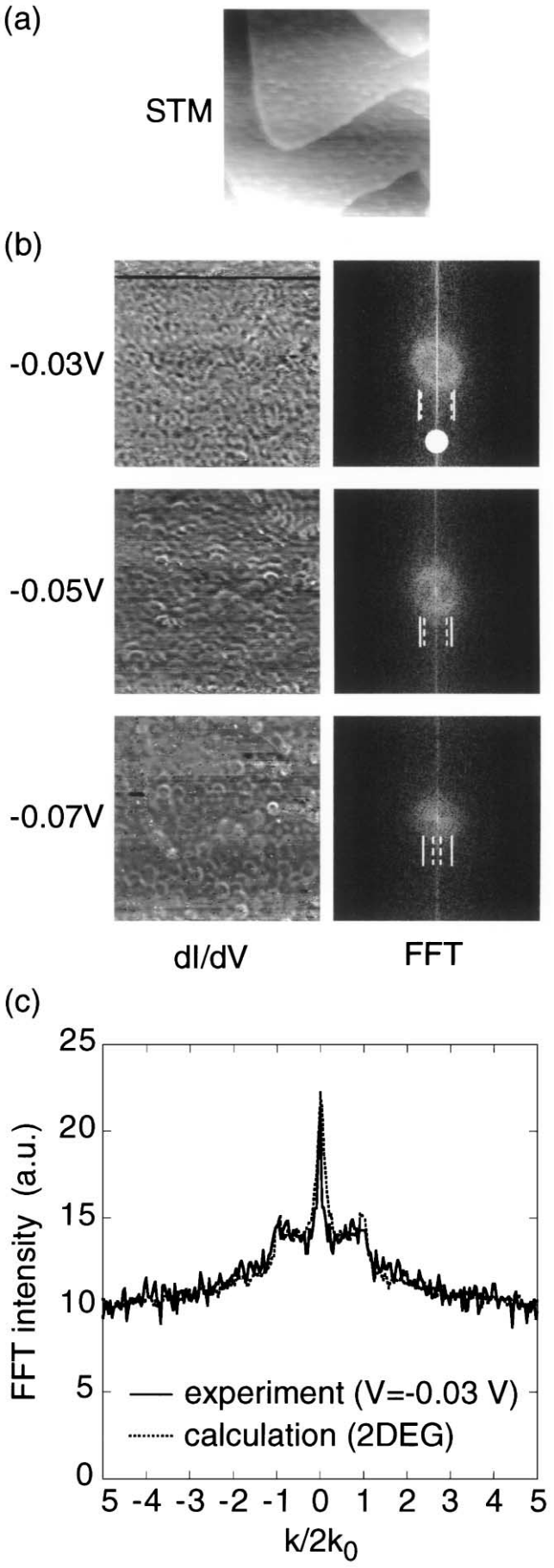

FIG. 2. (a) Constant current 268 nm × 268 nm STM and (b) dI/dV images obtained at $V < 0$ V (23.5 ± 5.5 K). The FFT pattern for each dI/dV image is also shown. Each pair of dashed (solid) lines in the FFT pattern indicates calculated peak widths $|4\mathbf{k}_\parallel|$ of 2DEG ground subband state in case I (case II). The expected spectrum for the 3DEG with the possible shortest $\lambda_{F,0}$ is shown by the filled circle in the FFT pattern. (c) Rotationally averaged FFT spectrum of the dI/dV image ($V = -0.03$ V) is compared with that of theoretical 2DEG LDOS ($k_0 = 2\pi/\lambda$, $\lambda = 22$ nm).

accumulation layer thickness z_a was 23 nm and $E_{F,\mathrm{InAs}}$ was 0.0077 eV above E_c (3DEG sheet carrier density $n = 2.6 \times 10^{11}$ cm^{-2}) in the center of the InAs layer. The 2DEG subband energies $E_{z,j}$ (carrier densities $N_{\mathrm{2DEG},j}$) were obtained for the ground state $E_{z,0} = -0.073$ eV ($N_{\mathrm{2DEG},0} = 1.2 \times 10^{12}$ cm^{-2}) and for the first excited state $E_{z,1} = -0.0083$ eV ($N_{\mathrm{2DEG},1} = 1.4 \times 10^{11}$ cm^{-2}) below $E_{F,\mathrm{InAs}}$. The surface electrons consist of more than 90% 2DEG and less than 10% 3DEG. We performed similar calculations for case II. Here, we ignored zero-dimensional confinement effects [13]. Experimental FFT spectra are crudely distributed around the calculated FFT spectrum peak of the 2DEG, though the calculation results using the possible shortest $\lambda_{F,0}$ of the 3DEG has smaller components. Moreover, since $k_\parallel$ ($= |\mathbf{k}_\parallel|$, $\mathbf{k}_\parallel$: the wave vector parallel to the surface) is a constant at a given energy E for 2DEG, this gives rise to the ring distribution in the FFT spectrum. This distribution becomes clearer at $V = -0.03$ V. We compared the FFT spectrum of the dI/dV image with that of the calculated 2DEG LDOS, considering the scatterers at the same positions in the STM image. It is confirmed that the FFT spectrum of the calculated 2DEG LDOS consistently reproduces the experimental spectrum [Fig. 2(c)]. These facts suggest that the observed corrugation patterns belong to 2DEG states.

The 2DEG LDOS at $V > 0$ V are similar to those at noble metal surfaces. This is because the perturbation by coexisting 3DEG LDOS becomes important. However, at $E \approx E_F$, we expect more dominant 2DEG feature at the InAs(111)A surface [where the 2DEG ($\leq 10^{12}$ cm^{-2}) coexists with the 3DEG ($\leq 10^{16}$ cm^{-3})] than at the noble metal surfaces (2DEG $\leq 10^{14}$ cm^{-2}, 3DEG $\leq 10^{23}$ cm^{-3} [14]).

Each equilateral triangle in the STM image [Fig. 3(a)] is a surface of stacking fault tetrahedron (SFT) [15]. The SFT is surrounded by the (111)A surface and three triangular {111}-stacking fault planes below the surface. Each intersection of the planes is a Lomer-Cottrell sessile (or Frank partial) dislocation [15]. The point defect (indicated by the arrow) arises due to a threading dislocation. These defects strongly scatter electron waves due to the locally different polarization in bonds and the charged dangling bonds. In the case of large SFT's with a side length much greater than electron wavelength λ, the SFT can effectively act as a two-dimensional quantum cage as $z_a \approx \lambda$. The corresponding dI/dV image in Fig. 3(a) shows the periodic peak arrangement within the triangles. The brighter regions are due to a higher LDOS. The pattern is similar to that observed within the triangular quantum corral [2]. Concentric circles are also imaged around the point defect. If V is increased, the period of the peaks becomes shorter [Fig. 3(b)].

When analysis is performed on the oscillation damping around the point defect, the damping factor is equivalent to $1/r$ (r: distance from point scatterer). This is equal to the damping of the 2DEG state scattering by a point scatterer [Fig. 3(c)]. We have confirmed stronger damping

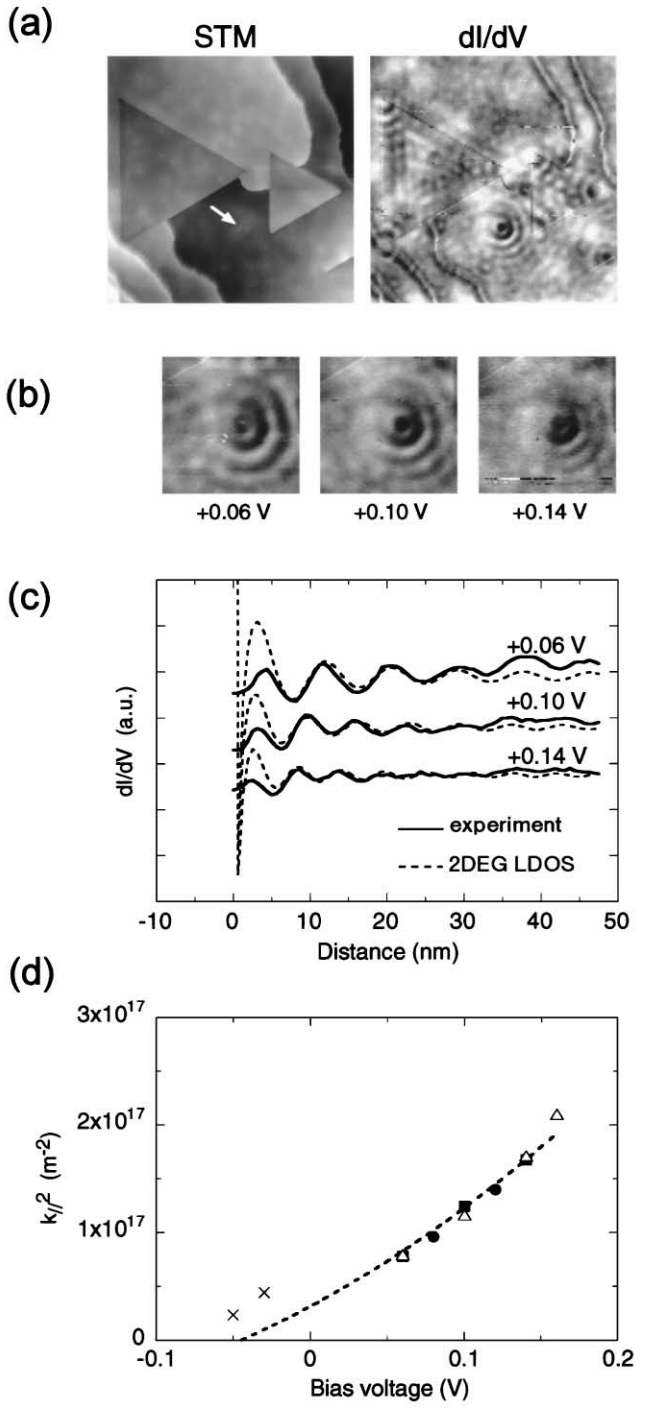

FIG. 3. (a) Constant current 214 nm $\times$ 214 nm STM image ($V = +0.10$ V) and the dI/dV image at 5.3 K. (b) dI/dV images around a point scatterer in 67 nm $\times$ 67 nm area and (c) oscillation profiles. Simulation curves are fitted assuming 2DEG LDOS oscillations $\propto \cos(2\mathbf{k}_\parallel \cdot \mathbf{r} + \delta)/r$ (δ is the scattering phase shift). We performed the fitting so that the simulation curves coincide with the measured value of the second nearest peak. (d) Bias voltage dependence of $k_\parallel^2$ around a point defect (filled squares) and within the SFTs (open triangles and filled circles). The $k_\parallel^2$ are obtained using FFT spectrum at $V < 0$ V (marked $\times$). The dashed curve is fitted considering a nonparabolicity ($m_0^* = 0.024 m_0$ at the $k_\parallel = 0$).

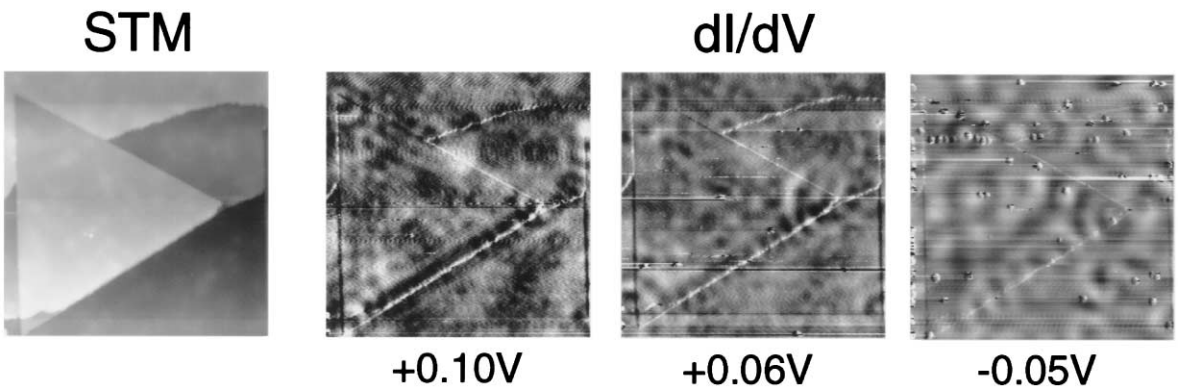

FIG. 4. Constant current 134 nm × 134 nm STM image of the SFT at 5.3 K. dI/dV images are mapped for occupied and unoccupied states.

for the 3DEG LDOS by calculation. A phase shift of about -0.95π indicates that the scatterer effectively behaves as a hard wall (phase shift $-\pi$).

The deviations in the present dI/dV signal map from the LDOS are very small [3]. We can therefore directly measure λ from the period of the dI/dV peaks (neglecting the nearest peak to the scatterer). Figure 3(d) shows the bias voltage dependence of $k_{\parallel}^2$ ($k_{\parallel} = 2\pi/\lambda$). In InAs, m^* is determined by E (or the electron density) due to the nonparabolic dispersion relation of the conduction band [6,11] expressed as $\hbar^2 k_{\parallel}^2/2m_0^* = E(1 + E/E_g)$. The measured $k_{\parallel}^2$ were well fitted using this nonparabolicity, whose curve shows $0 < k_{\parallel}$ at $V < 0$ V. The curve shows slightly smaller $k_{\parallel}^2$ than those derived from FFT analysis for occupied states, but E ($= E_F - 0.045$ eV) at $k_{\parallel} = 0$ is comparatively close to the $E_{z,0}$ position calculated above. This suggests that the 2DEG LDOS is reasonable to explain the continuous change of dI/dV images from positive to negative bias (Fig. 4).

The accumulated 2DEG must have a heavier m^* than the 3DEG at the same $E - E_{F,\mathrm{InAs}}$ because of shorter λ. For m^* at $E - E_{F,\mathrm{InAs}} = 0.1$ eV, we obtained $0.043m_0$. This value is consistent with m^* of the 2DEG in the accumulation layer [11], and is about 1.3 times as heavy as the reported m^* of 3DEG [6]. When we calculated m^* [6,16], we found that the corresponding m^* of the 2DEG is at least 1 (case II)–1.2 (case I) times as heavy as that of the 3DEG. We can therefore conclude that the observed standing waves belong to 2DEG states accumulated at the surface with a 3DEG LDOS as the background.

In summary, the characterization of 2DEG LDOS at the MBE-grown InAs(111)A surface was performed by using LT-STM. When dI/dV mapping was performed simultaneously with topography in the conduction band, wave phenomena were continuously observed. Periodic and symmetric patterns observed at point defects and inside SFT's show a nonparabolic dispersion relation. These features were consistently explained using LDOS of the two-dimensional subband state quantized in the surface accumulation layer.

We are grateful to Y. Tokura for helpful discussions. This study was partly supported by the NEDO collaboration program (NTDP-98) and the Japan Society for the Promotion of Science ("Research for Future" Program No. JSPS-RFTF96P00103). M. J. Butcher would like to thank EPSRC.

[1] J. Friedel, Philos. Mag. **43**, 153 (1952).
[2] M. F. Crommie, C. P. Lutz, D. M. Eigler, and E. J. Heller, Physica (Amsterdam) **83D**, 98 (1995), and references therein.
[3] J. Li, W.-D. Schneider, R. Berndt, and S. Crampin, Phys. Rev. Lett. **80**, 3332 (1998).
[4] O. Jeandupeux, L. Bürgi, A. Hirstein, H. Brune, and K. Kern, Phys. Rev. B **59**, 15 926 (1999).
[5] M. C. M. M. van der Wielen, A. J. A. van Roji, and H. van Kempen, Phys. Rev. Lett. **76**, 1075 (1996).
[6] R. Dombrowski, Chr. Wittneven, M. Morgenstern, and R. Wiesendanger, Appl. Phys. A **66**, S203 (1998).
[7] T. Yokoyama, M. Okamoto, and K. Takayanagi, Phys. Rev. Lett. **81**, 3423 (1998).
[8] H. Yamaguchi, M. R. Fahy, and B. A. Joyce, Appl. Phys. Lett. **69**, 776 (1996).
[9] L. Ö. Olsson, L. Ilver, J. Kanski, P. O. Nilsson, C. B. M. Andersson, U. O. Karlsson, and M. C. Håkansson, Phys. Rev. B **53**, 4734 (1996).
[10] G. R. Bell, T. S. Jones, and C. F. McConville, Appl. Phys. Lett. **71**, 3688 (1997).
[11] M. Morgenstern, Chr. Wittneven, R. Dombrowski, and R. Wiesendanger, Phys. Rev. Lett. **84**, 5588 (2000), and references therein.
[12] H. A. Washburn, J. R. Sites, and H. H. Wieder, J. Appl. Phys. **50**, 4872 (1979).
[13] R. Dombrowski, Chr. Steinebach, Chr. Wittneven, M. Morgenstern, and R. Wiesendanger, Phys. Rev. B **59**, 8043 (1999).
[14] P. Straube, F. Pforte, T. Michalke, K. Berge, A. Gerlach, and A. Goldmann, Phys. Rev. B **61**, 14 072 (2000).
[15] D. Hull and D. J. Bacon, *Introduction to Dislocations* (Pergamon, Oxford, 1984), Chap. 5.
[16] U. Merkt and S. Oelting, Phys. Rev. B **35**, 2460 (1987).